European Journal of Chemistry 2 (2) (2011) 152-157

European Journal of Chemistry

Journal homepage: www.eurjchem.com

Identification and characterization of geometrical isomeric photo degradation product of eprosartan using LC-MS and LC-NMR

Ravi Piyushkumar Shah, Archana Sahu and Saranjit Singh*

Department of Pharmaceutical Analysis, National Institute of Pharmaceutical Education and Research (NIPER), SAS Nagar 160062, Punjab, India

**Corresponding author at: Department of Pharmaceutical Analysis, National Institute of Pharmaceutical Education and Research (NIPER), Sahibzada Ajit Singh, Nagar 160062, Punjab, India. Tel.: +91.172.2214682; fax: +91.172.2214692. E-mail address: ssingh@niper.ac.in (S. Singh).*

COMMUNICATION INFORMATION

Received: 17 June 2010
Received in revised form: 02 November 2010
Accepted: 02 November 2010
Online: 30 June 2011

KEYWORDS

Eprosartan
Degradation behaviour
Photoisomerization
Geometric isomer
LC-MS
LC-NMR

ABSTRACT

The degradation of eprosartan was evaluated under ICH/WHO prescribed stress conditions. The drug degraded to only one product under photo alkali condition, whereas it was stable to conditions of hydrolysis, oxidation and thermal stress. The drug and its co-eluting product were well separated on RP-HPLC in a gradient mode. Subsequently, LC-MS/TOF and on-line H/D exchange studies were performed on both of them. The two showed same molecular mass, similar fragment ions and even the same number of labile hydrogens indicating the product to be an isomer of the drug. To confirm the same, ^{1}H and COSY LC-NMR studies were carried out by using an enriched sample. Distinguishing behaviour of chemical shifts proved the product to be (*Z*)-4-((2-butyl-5-(2-carboxy-3-(thiophen-2-yl)prop-1-enyl)-1*H*-imidazol-1-yl)methyl)benzoic acid. The structure was further supported by differential LC-MS ion intensities of the drug and the product.

1. Introduction

As per the International Conference on Harmonization (ICH) [1] and the World Health Organization (WHO) [2] stability test guidelines, stress studies and identification/ characterization of degradation product(s) are mandatory for new and existing drug molecules, respectively. Generally during stress and stability studies, the degradation products are generated in small quantities. So their characterization turns out to be a cumbersome process, when the conventional approach of isolation and spectral analysis is followed. Therefore, advanced hyphenated techniques, like LC-MS and LC-NMR, are being extensively explored for this purpose since the last few years [3-8].

Eprosartan is an angiotensin II receptor antagonist, which is used in the treatment of hypertension [9]. Although, the drug was approved by US-FDA in 1997 [10], only scant information on its degradation behaviour is known [11]. There is no report involving stress testing on the drug. Most of the literature texts cover development of HPLC and LC-MS methods for the determination of drug in different matrices [11-13]. Therefore, an endeavour of the present study was to: (*i*) degrade the drug under conditions of hydrolysis, oxidation, photolysis and thermal stress, as prescribed by ICH and WHO, (*ii*) separate the drug and the degradation product(s) on a LC column, (*iii*) obtain necessary spectral information for the generated degradation product(s) using LC-MS and LC-NMR, and (*iv*) characterize the degradation product(s) formed from the available data.

2. Experimental

2.1. Drug and reagents

Pure eprosartan was obtained as gratis sample from Ranbaxy Research Laboratories (Gurgaon, India). Analytical reagent (AR) grade sodium hydroxide (NaOH) was purchased from Ranbaxy Laboratories (S.A.S. Nagar, India), hydrochloric acid (HCl) from LOBA Chemie Pvt. Ltd. (Mumbai, India) and hydrogen peroxide (H_2O_2) from s.d. fine-chem Ltd. (Boisar, India). Buffer salts and all other chemicals were also of AR grade and bought from local suppliers. HPLC grade acetonitrile (ACN) and methanol (MeOH) were procured from J. T. Baker (Phillipsburg, NJ, USA). NMR grade ACN and deuterated water (D_2O) of 99.9% purity were obtained from Riedel-de Haen (Seelze, Germany) and Aldrich (California, Missouri, USA), respectively. ES Tuning Mix solution (Agilent Technologies, USA) was used as the MS/TOF calibrant. Water for HPLC studies was obtained from ultrapure water purification unit (Elga, Wycombe, England).

2.2. Apparatus and equipment

Precision water baths (Julabo, Seelbach, Germany) were used for hydrolytic studies. Thermal stress testing was carried out using a dri bath ((Thermolyne, Iowa, USA). The photostability chamber (KBWF 240, WTC Binder, Tuttlingen, Germany) was equipped with an illumination bank on the inside top, consisting of a combination of two UV (OSRAM L18 W/73) and four white fluorescent (PHILIPS TRULITE 18W/86) lamps, in accordance with Option 2 of the ICH guideline Q1B [14]. Both fluorescent and UV lamps were put on simultaneously. The samples were placed at a distance of 9 inches from the light bank. A lux meter (model ELM 201, Escorp, New Delhi, India) and a UV radiometer (model 206, PRC Krochmann GmbH, Berlin, Germany) were used to measure visible illumination and UV energy, respectively. Other equipments used for the study were sonicator (3210, Branson

ISSN 2153-2249 (Print) / ISSN 2153-2257 (Online)
DOI:10.5155/eurjchem.2.2.152-157.170

Ultrasoincs Corporation, CT, USA), precision analytical balance (AG 135, Mettler Toledo, Schwerzenbach, Switzerland), pH/Ion analyzer (MA 235, Mettler Toledo, Schwerzenbach, Switzerland) and autopipettes (Eppendorf, Hamburg, Germany).

The stand-alone HPLC system was VP series from Shimadzu (Kyoto, Japan) and was equipped with a photodiode array detector. It was controlled by SP1 software ver. 6.14. LC-MS/TOF results were obtained on a system in which LC (model 1100, Agilent Technologies, Waldbronn, Germany) was hyphenated to MicrOTOF-Q spectrometer (Bruker Daltonik, Bremen, Germany) using Hyphenation Star (version 3.1) and MicrOTOF Control (version 2.0) software. Multi-stage mass (MS^n) studies were carried out on a LTQ XL MS 2.5.0 system (Thermo, San Jose, USA). The same was controlled by Xcalibur (version 2.0.7 SP1) software. The MicrOTOF-Q instrument was also used for H/D exchange study on the drug, while LTQ XL system was employed for on-line H/D exchange investigations on the product. LC-NMR measurements were done using JNM-ECA 500 MHz spectrometer (JEOL, Tokyo, Japan) coupled to Prominence LC system (Shimadzu, Kyoto, Japan) and controlled by Delta (Version 4.3) and LC-NMR Dio (Version 2.0) software, respectively.

2.3. Stress testing

The stressors, choice of their concentration and preparation of samples were based on our previous publication [15]. As the drug was insoluble in water, it was dissolved in a mixture of ACN and water in a ratio of 50:50 (*v:v)* to achieve a stock concentration of 2 mg/mL. This stock was diluted 50:50 (*v:v)* with the stressor (e.g., HCl, water, NaOH or H_2O_2). Hydrolytic decomposition of the drug was carried out in 1 N HCl, water and 1 N NaOH at 80 °C for 48 h. The oxidative study was carried out in 15% *v/v* H_2O_2 at room temperature for 2 d. Photolytic studies on the drug in the solution state were carried out in 0.1 N HCl, water and 0.1 N NaOH by exposing the same for 13, 13 and 4 d, respectively, in a photostability chamber delivering 8500 lx of fluorescent and 0.5 W/m^2 of UV light and set at 40±1 °C/75±3% RH. Photolytic studies in the solid state were performed for 13 d by exposing a thin layer of the drug to light under the same conditions as in solution state. Parallel blank sets were kept in the dark for respective time points. For thermal stress testing, the drug was sealed in glass vials and placed in a thermostatic block at 50 °C for 21 d to see the effect of heat alone on the drug molecule. After subjecting to stress, samples were withdrawn at suitable time intervals and diluted four folds with ACN and water (50:50, *v:v*) before injection into HPLC.

2.4. HPLC method development

The LC column used in method development was Pursuit XRs C-8 (250 mm x 4.6 mm i.d., particle size 5 µm) from Varian (CA, USA). The ratios of organic modifier (ACN) and buffer (potassium dihydrogen phosphate (0.01 M; pH 3.0)) were varied in the mobile phase to separate the drug and degradation product(s). The buffer was prepared by dissolving 1.36 g of anhydrous potassium dihydrogen phosphate in 1L water and the pH was adjusted using phosphoric acid. The buffer pH was fixed as 3.0 considering the drug's pKa values of 3.1 and 4.3, calculated using ACD software. The mobile phase components were filtered through 0.45 µm nylon filter and degassed before use. The injection volume and flow rate were 10 µL and 1.0 ml/min, respectively. All studies were carried out at 25 ^oC. The wavelength of detection was 233 nm.

2.5. MS/TOF, MS^n and H/D exchange studies on the drug

MS/TOF studies were performed in ESI positive mode in the mass range of 50 to 1500 Da. The drug was also subjected to MS^n study, wherein fragmentation of various precursor ions was achieved using different collision energies. Mass system parameters were optimized appropriately for the above studies. H/D exchange was carried out on the MS/TOF system by direct injection of a drug solution (2 ppm) in ACN and D_2O (50:50, *v:v*).

2.6. LC-MS/TOF and on-line H/D exchange studies on the product

The drug and the stressed samples were subjected to LC-MS/TOF studies using the developed LC method, but after replacing phosphate buffer with ammonium acetate having same molarity and pH. For internal calibration, the ES Tuning Mix solution was injected through a diverter in a specific segment near the peak of interest. The on-line H/D exchange mass studies were carried out on the LTQ-MS^n system, wherein injection of D_2O was made via an additional channel, just before the peak of interest started eluting from the column. The flow of D_2O was continued until the peak was completely eluted.

2.7. LC-NMR studies on the drug and the product

For LC-NMR studies, the photolytic stressed sample was subjected to LC using the same mobile phase as used for HPLC, but using D_2O instead of water. The separated product was collected in the fraction loop using terminal cube and sent to inverse 3 mm NMR flow probe equipped with ^1H {^{13}C} channels with pulsed-field gradient along *z*-axis. The active sample volume of the probe was approximately 60 µl and the transfer time from UV cell to the active volume was 45 s at a flow-rate of 0.5 mL/min. One dimensional ^1H spectra were recorded using the WET pulse sequences for solvent suppression of ACN and residual HOD signal, with attenuated power at 64.5 [dB], which gave digital resolution of 0.76 Hz per point for the product. The spectra were acquired with 16 KHz spectral width, 16 K data points and 1024 scans. The drug solution (4 mg/mL) was prepared in the mobile phase and directly injected to LC-NMR probe. The COSY spectra of the drug and its product were acquired using WET pulse sequences for solvent suppression. A total of 96 scans were collected at 256 iterations in the F_1 dimension, using a spectral width of ~10 KHz in both dimensions. It was found that traces of methanol were present as an impurity in the mobile phase. Therefore, the chemical shifts of ^1H signals were referenced to the methoxy signal of the residual CH_3OH at δ 3.30 ppm.

3. Results and discussion

3.1. HPLC method

All the stressed solutions were initially analyzed by HPLC using ACN (A) and potassium dihydrogen phosphate (B) in the following same gradient mode: T_{min}/A:B; $T_{0\text{-}1}$/10:90; $T_{60\text{-}70}$/90:10; $T_{75\text{-}82}$/10:90. Except, frontal hump in the drug peak in alkali solution exposed to light, a sharp single drug peak was observed in all other stressed solutions. This indicated that the drug was stable to all the stress conditions except photo alkali. To separate the overlapping product in photo alkaline condition, the method was improved by varying the gradient. The desired resolution (Rs > 1.5) was achieved between the degradation product and the drug by using the gradient: T_{min}/A:B; $T_{0\text{-}4}$/18:82; T_{18}/29:71; T_{22}/30:70; T_{25}/18:82. The chromatogram in Figure 1 depicts the separation between the two components. During the course of studies, it was found that the degradation product was stable during sample handling and subsequent analysis.

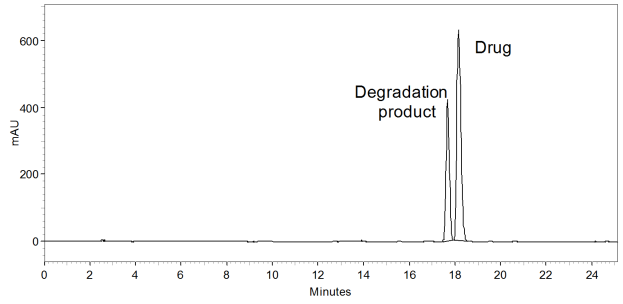

Figure 1. HPLC chromatogram showing separation of the drug and the product.

3.2. Optimized mass parameters

To get an optimal mass spectrum, the selected parameters for MS/TOF system were: end plate offset, -500 V; capillary voltage, -4500 V; nebuliser gas pressure, 1.2 Bar; dry gas flow, 6.0 L/min; dry temperature, 200 °C; funnel 1 RF, 150 Vpp; funnel 2 RF, 300 Vpp; ISCID energy, 0.0 eV; hexapole RF, 120 Vpp; quadrupole ion energy, 4.0 eV/Z; collision energy, 22.0 eV/z; transfer time, 50 µs; collision RF, 200 Vpp, and pre-pulse storage, 10 µs. Similarly, the tuned parameters for MS^n system were: capillary temperature, 300 °C; capillary voltage, 30 V; tube lens, 90 V; spray voltage, 5.0 kV, and sheath gas flow rate, 30 arb.

3.3. Mass fragmentation of the drug

MS/TOF spectrum of the drug showed sixteen fragments in total (Figure 2a; labelled a to p). Their accurate mass, possible molecular formula, exact theoretical mass, error in mmu, ring plus double bond (RDB) value and the number of labile hydrogen(s) determined from H/D exchange studies are given in Table 1. The MS^n data are listed in Table 2. These were employed to establish fragmentation pathway for the drug, as shown in Figure 3. Based on the possibilities of protonation in the drug structure, four routes were assigned for its fragmentation. The first two were inter-related, and proceeded with subsequent losses of H_2O or CO to generate fragments of *m/z* 407, *m/z* 389, *m/z* 379 and *m/z* 361. The third and major route was initiated by the loss of thiophene, yielding a fragment of *m/z* 341 that was further reduced to ions of *m/z* 297 and *m/z* 207 through neutral loss of CO_2 and $C_8H_6O_2$, respectively. Both these ions further produced a fragment of *m/z* 163 by respective neutral losses of $C_8H_6O_2$ and CO_2. The fourth route, which involved protonation of imidazole ring, cleaved the drug into two major fragments of *m/z* 291 and *m/z* 135 and a minor of *m/z* 290. The ion of *m/z* 291 first lost H_2O and then CO to yield daughters of *m/z* 273 and *m/z* 245, respectively. The pathway *m/z* 290 → *m/z* 272 → *m/z* 244 involved loss of the substituted phenyl moiety without hydrogen transfer to the imidazole ring, which could only be justified through the formation of radical cations.

3.4. LC-MS/TOF and on-line H/D exchange studies

LC-MS/TOF studies on the drug (Figure 2a) and its product (Figure 2b) showed the latter to have the same mass profile as that of the drug. The calculated chemical formula for each fragment (Table 1) was also same for the both. Even on-line H/D exchange studies showed the same molecular mass of *m/z* 428 for the drug and the product, indicating same number of the labile hydrogens. The only difference was in relative fragment ion intensities in MS/TOF spectra (Figure 2), which was seen even on repeated injections. While the ion of *m/z* 207 (53.1%) was most prominent in case of the drug, the same was very low abundant (3.1%) in the degradation product. A similar situation existed for the fragment of *m/z* 341. Conversely, abundance of the fragment of *m/z* 273 was higher in the product (43.5%) than the corresponding ion in case of the drug (6.8%).

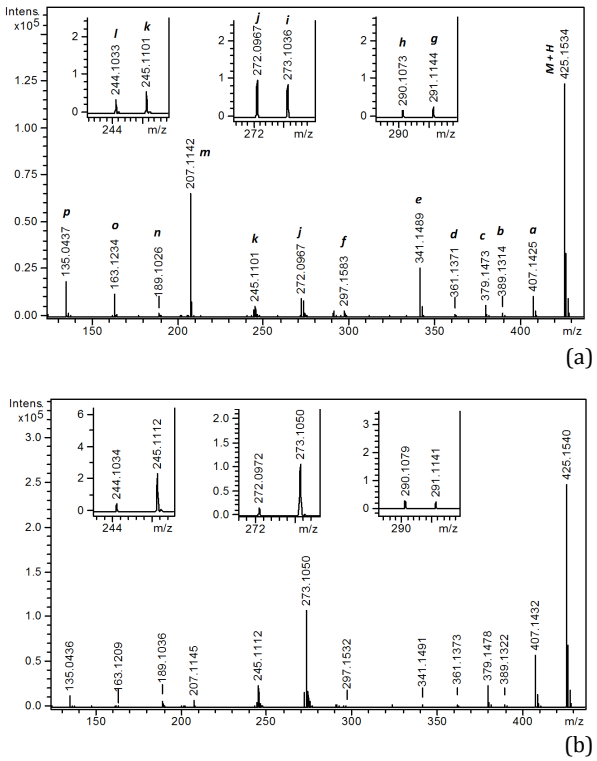

Figure 2. LC-MS/TOF spectrum of the drug (a) and the product (b); The labels a-p are for different fragments of the drug. The same apply even to the fragments for the product in lower figure b.

3.5. LC-NMR study

^{1}H LC-NMR spectra of the drug and the product are shown in Figure 4. The corresponding ^{1}H peak assignments along with multiplicity and coupling constants, and COSY correlations are given in Table 3. The prominent peaks for the drug included: (*i*) two doublets at δ 7.95 and δ 7.16 ppm arising due to two aromatic resonances corresponding to the positions H-9,11 and H-8,12, respectively; (*ii*) two singlets arising from H-5 and H-13 at δ 7.58 and δ 7.35 ppm, respectively; (*iii*) three aromatic resonances (two doublets, one multiplet) arising due to thiophene ring corresponding to H-18, H-20 and H-19 at δ 7.22, δ 6.65 and δ 6.90 ppm, respectively; (*iv*) two singlets corresponding to methylene protons for position H-6 and H-15 at δ 5.50 and δ 3.96 ppm, respectively, and (*v*) two triplets corresponding to methyl and methylene protons arising at δ 0.78 and δ 2.97 ppm for H-4' and H-1', respectively, and two multiplets arising at δ 1.26 and δ 1.55 ppm (H-3' and H-2') representing the methylene protons of the butyl chain. Further COSY data (Table 3) also supported the peak assignments. The ^{1}H LC-NMR of the product showed only one major dissimilar peak (δ 5.57 ppm) when compared to the drug (δ 7.35 ppm). Other ^{1}H peaks were insignificantly changed, while COSY correlations were the same to the drug (Table 3).

3.6. Structure elucidation

As discussed above, identical molecular ion mass and similar fragmentation profile in LC-MS study revealed that the product was an isomer of the drug. This was verified through distinguishing spectral difference in LC-NMR spectra.

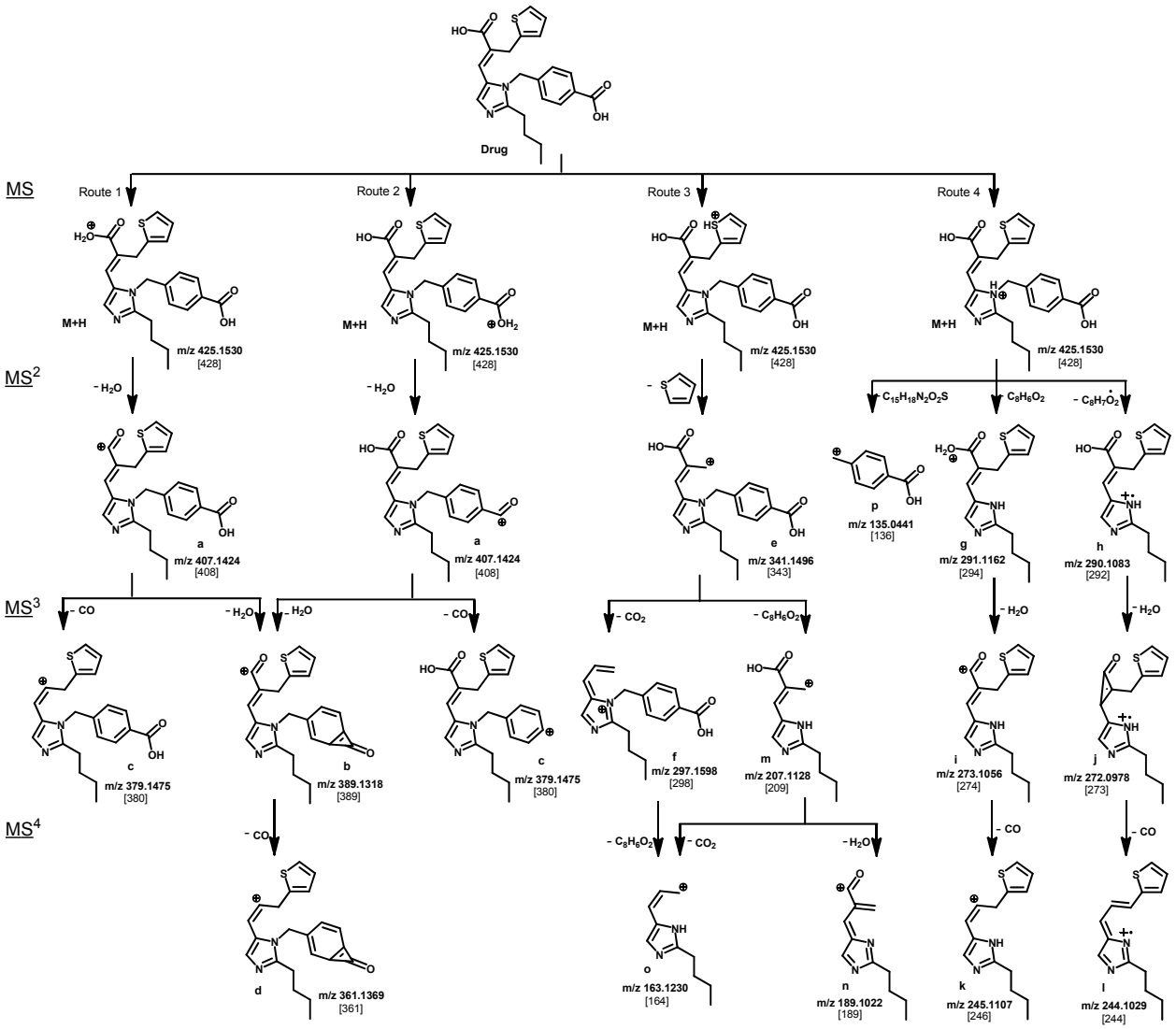

Figure 3. Proposed mass fragmentation pattern of the drug. The value of calculated accurate mass is shown below each structure, along with the mass obtained in H/D exchange study (in brackets).

The observed upfield behaviour of H-13 in the product, (Table 3) indicated that the surroundings of vinyl H-13 had changed significantly. This was only possible if the drug (*E* form) was converted to *Z* isomer. Due to this geometric isomerization, d-orbital electrons of sulfur showed shielding effect to vinyl H-13. Moreover, observed minor change in *J* value of H-18 might be due this spatial non-bonding interaction. The supposition of isomerization was verified through correlation of the observed differential MS peak intensities of the drug and the product (Figure 2a and 2b), considering that isomers are known to show different fragment ion intensities [16,17].

As discussed under Section 3.4, the intensity of mass peaks of *m/z* 207 and *m/z* 341 were significantly less in case of the product. This was perhaps due to hindered protonation of thiophene ring system by spatial non-bonding interaction of sulphur and vinyl hydrogens. In this circumstance, fragmentation from other site (route four; N3-C6; Figure 3) could be preferred, and this phenomenon was clearly seen from the observed higher intensity of the ion of *m/z* 273 for the product. Incidentally, a similar observation was made by Brum *et al.* in MS study on *E* and *Z* isomers of eprosartan carried out in APCI mode through direct injection [18]. This further strengthens the identity of degradation product formed in photo alkali condition as discussed above.

The elucidated structure is further supported by the mechanism of isomerization, outlined in Figure 5. It is postulated that eprosartan (*E*-isomer) is converted to *Z*-isomer under photo alkali condition through ionization of carboxyl group, which stabilizes the radical formed during the transition state. The geometrical conversion (*cis* to *trans*) of vinyl compounds on exposure to light is known previously [19,20].

4. Conclusion

This systematic stress degradation study on eprosartan, carried out according to ICH/WHO guidelines, reveals that the drug is stable to hydrolysis, oxidation, thermal stress and even to light in solid state and in neutral and acid solutions. It is only unstable in photo alkaline solutions. The degradation product is characterized through complementary use of hyphenated LC-MS and LC-NMR techniques as *Z*-isomer of the drug ((*Z*)-4-((2-butyl-5-(2-carboxy-3-(thiophen-2-yl)prop-1-enyl)-1H-

Table 1. MS/TOF data and relative ion intensities of the drug and the product along with MS^n and on-line H/D exchange data for the drug.

Peak no.	MS/TOF data and relative ion intensity of drug (of product)	Best possible molecular formula	Exact mass of most probable structure	Error in mmu for drug (for product)	RDB	Possible parent fragment	Difference from parent ion	Molecular formulae for the best two possible losses		Mass values after H/D exchange	Number of labile hydrogens
								Loss 1	Loss 2		
$[M+H]^+$	425.1534; 100 (425.1540; 100)	$C_{23}H_{25}N_2O_4S$	425.1530	0.4 (1.0)	12.5	-				428	3
a	407.1425; 8.8 (407.1432; 23.2)	$C_{23}H_{23}N_2O_3S$	407.1424	0.1 (0.8)	13.5	$[M+H]^+$	18.0106	H_2O		408	1
b	389.1314; 1.2 (389.1322; 1.0)	$C_{23}H_{21}N_2O_2S$	389.1318	-0.4 (0.4)	14.5	a	18.0106	H_2O		389	0
c	379.1473; 5.0 (379.1478; 9.5)	$C_{22}H_{23}N_2O_2S$	379.1475	-0.2 (0.3)	12.5	a	27.9951	CO	N_2	380	1
d	361.1371; 1.0 (361.1373; 0.8)	$C_{22}H_{21}N_2OS$	361.1369	0.2 (0.4)	13.5	b	27.9951	CO	N_2	361	0
e	341.1489; 20.7 (341.1491; 0.7)	$C_{19}H_{21}N_2O_4$	341.1496	-0.7 (-0.5)	10.5	$[M+H]^+$	84.0038	C_4H_4S	$C_3H_2NO_2$	343	2
f	297.1583; 2.7 (297.1532; 0.2)	$C_{18}H_{21}N_2O_2$	297.1598	-1.4 (-6.5)	9.5	e	43.9904	CO_2	N_2O	298	1
g	291.1144; 2.2 (291.1141; 1.0)	$C_{15}H_{19}N_2O_2S$	291.1162	-1.8 (-2.0)	7.5	$[M+H]^+$	134.0379	$C_8H_6O_2$	$C_5H_{10}O_2S$	294	3
h	290.1073; 1.5 (290.1079; 1.2)	$C_{15}H_{18}N_2O_2S$	290.1083	-1.0 (-0.4)	8.0	$[M+H]^+$	135.0451	$C_8H_7O_2$	$C_5H_{11}O_2S$	292	2
I	273.1036; 6.8 (273.1050; 43.5)	$C_{15}H_{17}N_2OS$	273.1056	-2.0 (-0.6)	8.5	g	18.0108	H_2O		274	1
J	272.0967; 7.9 (272.0972; 6.6)	$C_{15}H_{16}N_2OS$	272.0978	-1.1 (-0.6)	9.0	h	18.0101	H_2O		273	1
k	245.1101; 4.6 (245.1112; 9.5)	$C_{14}H_{17}N_2S$	245.1107	-0.6 (0.5)	7.5	i	27.9933	CO	N_2	246	1
l	244.1033; 2.7 (244.1034; 2.1)	$C_{14}H_{16}N_2S$	244.1029	-0.4 (0.5)	8.0	j	27.9941	CO	N_2	244	0
m	207.1142; 53.1 (207.1145; 3.1)	$C_{11}H_{15}N_2O_2$	207.1128	1.4 (1.7)	5.5	e	134.0333	$C_8H_6O_2$	$C_3H_6N_2O_4$	209	2
n	189.1026; 1.2 (189.1036; 2.4)	$C_{11}H_{13}N_2O$	189.1022	0.4 (1.4)	6.5	m	18.012	H_2O		189	0
o	163.1234; 9.8 (163.1209; 0.6)	$C_{10}H_{15}N_2$	163.1230	-0.4 (-2.1)	4.5	m	43.9915	CO_2	N_2O	164	1
p	135.0437; 14.9 (135.0436; 4.8)	$C_8H_7O_2$	135.0441	-0.3 (-0.4)	5.5	$[M+H]^+$	290.1086	$C_{15}H_{18}N_2O_2S$	$C_{15}H_{18}N_2O_4$	136	1

a-h: peak numbers shown in Figure 2a.

Table 2. MS^n fragmentation of the drug.

MS^n	Precursor ion	Product ions
MS^2	425	407, 379, 361, 341, 291, 290, 207, 135
MS^3	407	389, 379, 361
	341	297, 207, 189, 163
	291	273, 245
	290	272, 244
MS^4	389	361
	297	163
	207	189, 163
	273	245

Table 3. ^1H LC-NMR peak assignments of the drug and the product along with multiplicity, coupling constants and COSY data.

Position	Drug		Product	
	δH/ppm (Multiplicity, *J* value in Hz)	COSY	δH/ppm (Multiplicity, *J* value in Hz)	COSY
5	7.58 (s)	-	7.48 (s)	-
6	5.50 (s)	-	5.34 (s)	-
8	7.16 (d, 7.64)	H-9	7.11 (d, 7.64)	H-9
9	7.95 (d, 7.64)	H-8	7.96 (d, 7.64)	H-8
11	7.95 (d, 7.64)	H-12	7.96 (d, 7.64)	H-12
12	7.16 (d, 7.64)	H-11	7.11 (d, 7.64)	H-11
13	7.35 (s)	-	5.57 (s)	-
15	3.96 (s)	-	3.79 (s)	-
18	7.22 (d, 5.35)	H-19	7.12 (d, 4.59)	H-19
19	6.90 (m)	H-18, H-20	6.90 (m)	H-18, H-20
20	6.65 (d, 3.06)	H-19	6.74 (d, 3.06)	H-19
1'	2.97 (t, 7.64)	H-2'	2.94 (t, 7.64)	H-2'
2'	1.55 (m)	H-1', H-3'	1.57 (m)	H-1', H-3'
3'	1.26 (m)	H-2', H-4'	1.28 (m)	H-2', H-4'
4'	0.78 (t, 7.64)	H-3'	0.80 (t, 7.64)	H-3'

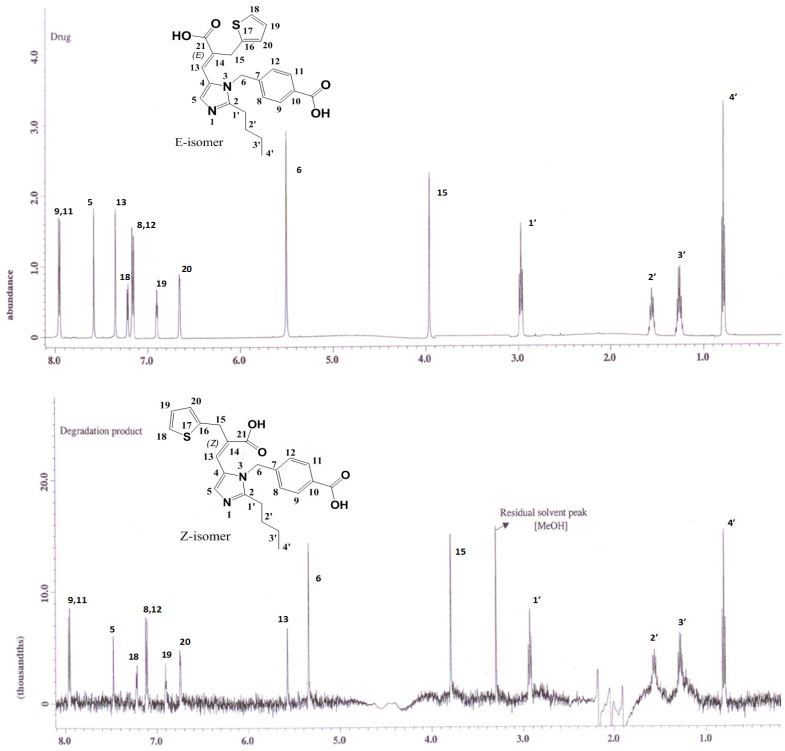

Figure 4. ^{1}H LC-NMR spectra of the drug (upper) and the product (lower).

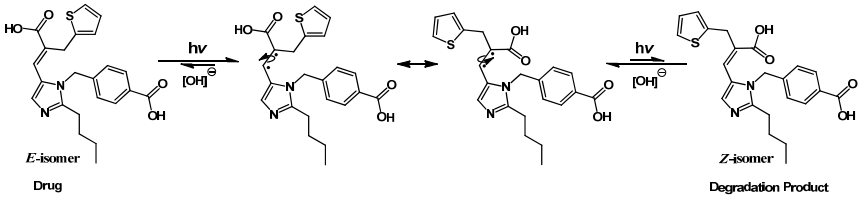

Figure 5. Mechanism of formation of *Z*-isomer from the drug.

imidazol-1-yl)ethyl)benzoic acid). Though it is a reported photolytic product of eprosartan, the exact condition under which it is formed from the drug under light is identified here. The mechanism of formation of the product is proposed. A complete mass fragmentation pathway of the drug is reported for the first time. Also, extensive MS and NMR data and their interpretation are provided for both the drug and the degradation product. The given information can be gainfully exploited in future investigations on characterization of process related impurities, drug-excipient interaction products, and/or metabolites of the drug. Overall, the study strengthens the utility of hyphenated tools for characterizing the unknown products formed in small quantities during stability or stress studies, against the use of cumbersome procedure of isolation or synthesis.

References

[1]. ICH Topic Q1A (R2), Stability Testing of New Drug Substances and Products, in: International Conference on Harmonisation, IFPMA, Geneva, 2003.

[2]. WHO, Draft Stability Testing of Active Pharmaceutical Ingredients and Pharmaceutical Products, World Health Organization, Geneva, 2007.

[3]. Murakami, T.; Kawasaki, T.; Takemura, A.; Fukutsu, N.; Kishi, N.; Kusu, F. *J. Chromatogr. A* **2008**, *1208*, 164-174.

[4]. Shah, R. P.; Kumar, V.; Singh, S. *Rapid Commun. Mass Spectrom.* **2008**, *22*, 613-622.

[5]. Novak, P.; Tepes, P.; Ilijas, M.; Fistric, I.; Bratos, I.; Avdagic, A.; Hamersak, Z.; Markovic, V. G.; Dumic, M. *J. Pharm. Biomed. Anal.* **2009**, *50*, 68-72.

[6]. Dev, R. V.; Kiran, G. S. U.; Subbaiah, B. V.; Babu, B. S.; Babu, J. M.; Dubey, P. K.; Vyas, K. *Magn. Reson. Chem.* **2009**, *47*, 443-448.

[7]. Shah, R. P.; Sahu, A.; Singh, S. *J. Pharm. Biomed. Anal.* **2010**, *51*, 1037-1046.

[8]. Shah, R. P.; Singh, S. *J. Pharm. Biomed. Anal.* **2010**, *53*, 755-761.

[9]. Hoffman, B. B. in: Brunton, L.L. Goodman & Gilman's The Pharmacological Basis of Therapeutics, 11th Edition, McGraw-Hill, 859-860, 2006.

[10]. Available at: http://www.accessdata.fda.gov/scripts/cder/drugsatfda/index.cfm? Fuseaction=Search.DrugDetails (accessed on 11 April 2011).

[11]. Hsu, L. C. *J. Liq. Chrom. & Rel. Technol.* **1998**, *21*, 1685-1700.

[12]. Xue-Ning, L.; Hong-Rong, X.; Wei-Li, C.; Gang-Yi, L.; Nan-Nan. C.; Chen Y. *J. Chromatogr. B* **2007**, *853*, 47-53.

[13]. Ferreirós, N.; Iriarte, G.; Alonsoa, R. M.; Jiménez, R. M.; Ortíz, E. *J. Chromatogr. A* **2006**, *1119*, 309-314.

[14]. ICH Topic Q1B, Stability Testing: Photostability Testing of New Drug Substances and Products, in: International Conference on Harmonisation, IFPMA, Geneva, 1996.

[15]. Bakshi, M.; Singh, S. *J. Pharm. Biomed. Anal.* **2002**, *28*, 1011-1040.

[16]. Mayer-Helm, B.; Hofbauer, L.; Pani, J. *J. Mass. Spectrom.* **2010**, (Article in Press; doi:10.1002/jms.1757).

[17]. Ge, G. B.; Zhang, R.; Ail, C. Z.; He Y. Q.; Zhang Y. Y.; Liu X. B.; Yang L.; Wang Z. T.; Yang L. *Rapid Commun. Mass Spectrom.* **2009**, *23*, 425-432.

[18]. Brum, J.; Hannah, R. *Rapid Commun. Mass Spectrom.* **1997**, *11*, 1430-1434.

[19]. Thoma, K.; Kuebler, N.; Reimann, E. *Pharmazie* **1997**, *52*, 362-373.

[20]. Albini, A.; Fasani, E. in: Tønnesen H. H. The Photostability of Drugs and Drug Formulations, 2nd Edition, Taylor and Francis, 69-71, 2004.